SCIENTIFIC REPORTS

OPEN

SUBJECT AREAS:
DRUG DELIVERY
GENE DELIVERY

Received
13 August 2014

Accepted
29 October 2014

Published
17 November 2014

Correspondence and requests for materials should be addressed to Y.Y.L. (liuyiyao@hotmail.com)

* These authors contributed equally to this work.

Multifunctional Core/Shell Nanoparticles Cross-linked Polyetherimide-folic Acid as Efficient Notch-1 siRNA Carrier for Targeted Killing of Breast Cancer

Hong Yang[1]*, Ying Li[1]*, Tingting Li[1], Min Xu[1], Yin Chen[1], Chunhui Wu[1], Xitong Dang[2] & Yiyao Liu[1]

[1]Department of Biophysics, School of Life Science and Technology, University of Electronic Science and Technology of China, Chengdu 610054, Sichuan, P.R. China, [2]Division of Trauma, Surgical Critical Care and Burns, University of California San Diego, CA 92103, USA.

In gene therapy, how genetic therapeutics can be efficiently and safely delivered into target tissues/cells remains a major obstacle to overcome. To address this issue, nanoparticles consisting of non-covalently coupled polyethyleneimine (PEI) and folic acid (FA) to the magnetic and fluorescent core/shell of Fe_3O_4@SiO_2(FITC) was tested for their ability to deliver Notch-1 shRNA. Our results showed that Fe_3O_4@SiO_2(FITC)/PEI-FA/Notch-1 shRNA nanoparticles are 64 nm in diameter with well dispersed and superparamagnetic. These nanoparticles with on significant cytotoxicity are capable of delivering Notch-1 shRNA into human breast cancer MDA-MB-231 cells with high efficiency while effectively protected shRNA from degradation by exogenous DNaseI and nucleases. Magnetic resonance (MR) imaging and fluorescence microscopy showed significant preferential uptake of Fe_3O_4@SiO_2(FITC)/PEI-FA/Notch-1 shRNA nanocomplex by MDA-MB-231 cells. Transfected MDA-MB-231 cells exhibited significantly decreased expression of Notch-1, inhibited cell proliferation, and increased cell apoptosis, leading to the killing of MDA-MB-231 cells. In light of the magnetic targeting capabilities of Fe_3O_4@SiO_2(FITC)/PEI-FA, our results show that by complexing with a second molecular targeting therapeutic, such as Notch-1 shRNA in this report, Fe_3O_4@SiO_2(FITC)/PEI-FA can be exploited as a novel, non-viral, and concurrent targeting delivery system for targeted gene therapy as well as for MR imaging in cancer diagnosis.

RNA interference (RNAi), a powerful technology for sequence-specific gene silencing, has been widely used in silencing many important oncogenes that play major roles in various stages of tumor development including cell transformation, unrestricted tumor cell proliferation and metastasis[1,2]. However, efficient delivery of small interfering RNA (siRNA) to targeted sites remain a major hurdle to overcome owing to the rapid degradation by serum nucleases, hepatic clearance, low transfection efficiency, off-target effect, and inefficient release from endosomes[2,3]. Generally, there are two major nucleic acid delivery systems, viral and nonviral systems. The viral vector generally has high efficiency in delivery, but the lack of tissue/cell targeting ability, cytotoxicity, immunogenicity, and limited capacity to accommodate large inserted genetic materials should be considered when used *in vivo*. Non-viral nano-carrier gene delivery systems, such as liposomes, nano-hydrogel, biodegradable nanoparticles, and inorganic nanoparticles, generally have lower transfection efficiency compared to their viral counterparts. However, because these non-viral nano-carriers possess low immunogenicity, low cytotoxicity, ease of manipulation, their transfection efficiency and formulations have been significantly optimized to meet the requirements for gene delivery. Although siRNA can now be easily delivered into cultured cells by viral or non-viral approaches, targeted delivery *in vivo* remains a big challenge in cancer gene therapy. Inorganic nanoparticles such as Fe_3O_4 may become an ideal siRNA carrier *in vivo* owing to its nano-sized particles for crossing physiological barriers and its potential for various surface modifications that can be used for targeted delivery.

In the last two decades, there has been an ever-increasing interest in fabricating nanometer-scale carriers for drug or gene delivery. Among them, superparamagnetic iron oxide nanoparticle (SPIO), for instance, Fe_3O_4 nanoparticle, is a promising candidate for their unique magnetic property, large surface area, and low cytotoxicity. However, two limitations need to be surpassed before they can be used as an efficient drug/gene delivery system. One is few functional groups on their surfaces, and the other is low dispersity and easy to aggregate or deposit. These limitations could largely be overcome by surface coating of the magnetic nanoparticles. Silica is one of the exceptional coating materials for encapsulating magnetic nanoparticles because of its good biocompatibility, excellent physicochemical stability, and its ease of surface multi-functionalization. In general, silica coating can be achieved by the Stöber process or the reverse (water-in-oil) microemulsion method[3–6]. These silica-coated fluorescent magnetic nanoparticles have been widely used to develop biomedical platforms for simultaneous imaging, diagnosis, and therapy. However, fabricating a desirable outer surface that can be further modified by adding another functional group or a targeting moiety remains challenging.

For nucleic acid, for instance, siRNA delivery, the silica surface charge should be positive. Introducing cationic charge on inorganic materials typically involve surface grafting with amine groups and coating with cationic polymers through either covalent or electrostatic association. These positively charged nanoparticles have been demonstrated to be able to carry nucleic acids and can be used an alternative to traditional viral vectors[7]. Polyethyleneimine (PEI), which contains primary, secondary, and tertiary amines to complex with nucleic acids such as DNA or siRNA, is one of the most widely studied cationic polymers for gene delivery. In addition, PEI can be easily modified by coupling some small molecules to endow it specific targeting ability. PEI can also induce cytotoxicity at high molecular weight and in high concentration, which is usually not the case in its application as a nanoparticle carrier[8].

Efficient targeted delivery of therapeutics is an important aspect to consider when designing targeting nanoparticles for cancer gene therapy. Insufficient uptake by targeted tissues will decrease the therapeutic benefit and affect the quality of imaging, which at the same time may increase the concentration of the therapeutics at the off-target sites and thus increasing the toxic side effects. One way to increase the local concentration of nanotherapeutics in tumor tissue is to conjugate these nanoparticles with targeting molecules that have high affinity to targeted tumor cells[9]. Folic acid (FA), a nonimmunogenic ligand, has emerged as an attractive specific targeting molecule for anticancer drug delivery because folate receptors are often overexpressed on the surface of many human cancers including ovarian, lung, breast, endometrial, renal, and colon cancers[10–13]. This folate receptor-mediated targeting has also been used as an imaging probe for cancer diagnosis[14]. Folate ligand is expected to gain popularity as a targeting molecule in tumor theranostics because of its simple and well-defined conjugation chemistry.

Accumulating evidence showed that Notch signal pathway played a key role in normal development and was increasingly recognized for its importance in cancer biology[14,15]. In mammalian, Notch pathway includes four transmembrane receptors (Notch-1 to 4) and five ligands (Delta-like 1, 3, 4, Jagged 1, 2). Upon activation, Notch-1 was cleaved by γ-secretase and released the Notch-1 intracellular domain (NICD) from the plasma membrane. NICD then translocates into the nucleus of the cells, where it formed a complex with transcriptional factors that regulated the expression of target genes and leading to altered cellular behaviors. Aberrant Notch signaling has been demonstrated to facilitate the proliferation and survival of tumor cells by regulating downstream effectors or other signaling pathways. Hence, targeting Notch signaling pathway is a promising treatment option for cancer.

In this study, a magnetic and fluorescent core/shell nanoparticles-based Notch-1 shRNA delivery system (denoted as Fe_3O_4@SiO_2(FITC)/PEI-FA/Notch-1 shRNA) was created, where FA was conjugated to PEI to increase its targeting capacity. The physiochemical characteristics of the Fe_3O_4@SiO_2(FITC)/PEI-FA/Notch-1 shRNA nanocomplex were analyzed by agarose gel electrophoresis, nuclear magnetic resonance spectra, and zeta potential measurements. The *in vitro* cytotoxicity, biocompatibility, cellular uptake efficiency, intracellular biodistribution, and the effects on cell proliferation and apoptosis in human breast cancer MDA-MB-231 cells upon treatment with the nanocomplex were extensively evaluated. We found this new sub-100 nm nanocomplexes exhibited low cytotoxicity, excellent colloidal stability in dilute aqueous dispersions, good biocompatibility, the ability to shield the loaded shRNA from nuclease degradation, and efficient targeted delivery of Notch-1 shRNA. We further demonstrated that the fabricated multifunctional Fe_3O_4@SiO_2(FITC)/PEI-FA/Notch-1 shRNA nanocomplex possesses magnetic properties that could be used as magnetic imaging probes at cellular level. The multifunctional nanocomplex has the potential to be exploited as a theranostics for targeted cancer gene therapy and MR imaging for cancer diagnosis.

Methods

Materials and chemicals. Tetraethylorthosilicate (TEOS), 3-aminopropyltrimethoxysilane (APS), fluorescein isothiocyanate (FITC), branched polyethyleneimine (PEI, 25 kD), *N,N′*-Dicyclohexylcarbodiimide (DCC), and *N*-hydroxysuccinimide (NHS) were obtained from Sigma-Aldrich (St Louis, MO, USA). Iron oxide nanoparticles (10 nm) were obtained from Nanjing Emperor Nano Material Co, Ltd (Nanjing, China). L15 cell culture medium, fetal bovine serum (FBS), and trypsin were purchased from Gibco (Grand Island, NY, USA). Folic acid (FA) was obtained from Alexis (Los Angeles, CA, USA). Trizol and calcein-AM were from Invitrogen (Carlsbad, CA, USA). Rabbit anti-human Notch-1 polyclonal antibody was purchased from Cell Signaling Technology (Boston, MA, USA). All chemicals were used as received without further purification.

Synthesis of Fe_3O_4@SiO_2(FITC)/PEI-FA/Notch-1 shRNA nanocomplex. Fe_3O_4@SiO_2(FITC) was prepared following a previously described procedure with some minor modifications[4,16,17]. Briefly, 2 mg of FITC was mixed with 125 μl of APS in 1 mL of anhydrous ethanol in the dark and allowed to react at room temperature for 24 h. The resulting mixture of FITC-APS conjugates in solution was then stored at 4°C. One milliliter of aqueous solution containing magnetic particles was diluted with 1 mL of water and 7.5 mL of anhydrous ethanol. Fifty microliters of TEOS and 200 μl of ammonia solution (28–30% by NH3) were added to this reaction mixture containing magnetic particles while stirring at 300 rpm for 24 h at room temperature, followed by FITC-APS solution addition with continuous stirring for 48 h. The reaction was terminated by adding methanol. The Fe_3O_4@SiO_2(FITC) nanoparticles were harvested by centrifugation at 12,000 rpm for 5 min and washed five times with deionized water to remove excess reactants.

To noncovalently couple Notch-1 shRNA to the surface of the Fe_3O_4@SiO_2(FITC) nanoparticles, co-polymer of PEI-FA were synthesized as follows: FA was activated in the presence of DCC and NNS by gentle stirring (300 rpm) for 12 h at room temperature (25°C), followed by addition of PEI to allow for another 12 h gentle stirring. The reaction mixture was then dialyzed for 48 h against deionized water to remove any unreacted reactants. The PEI-FA solution was added to the Fe_3O_4@SiO_2(FITC) nanoparticle suspension (1 ml), which were then mixed by rotating for 2 h at a speed of 180 rpm to allow PEI-FA to graft onto the surface of Fe_3O_4@SiO_2(FITC) nanoparticles. Unbound PEI-FA was removed by centrifugation at 10,000 rpm for 5 min with deionized water for three times. Notch-1 shRNA was incubated in the Fe_3O_4@SiO_2(FITC)/PEI-FA suspension for 30 min at room temperature to form Fe_3O_4@SiO_2(FITC)/PEI-FA/Notch-1 shRNA nanocomplex by electrostatic absorption at various weight ratios. The synthetic procedure for the Fe_3O_4@SiO_2(FITC)/PEI-FA/Notch-1 shRNA nanocomplex is summarized in Figure 1.

Characterization of nanocomplex. The size and morphology of the nanoparticles were examined by transmission electron microscopy (TEM) (JEM-100CX, JEOL, Tokyo, Japan) and scanning electron microscopy (SEM) (JSM-6490LV, JEOL, Tokyo, Japan). An aqueous dispersion of the nanoparticles was drop-cast onto a carbon-coated copper grid, and the grid was air-dry at room temperature before loading into the microscope. The presence of Fe_3O_4 and silica shell in the nanoparticles was evidenced by energy-dispersive X-ray (XRD) analysis. The zeta potential and the particle size distributions were determined using laser dynamic light scattering with Mastersizer 2000 (Malvern Instruments, Malvern, UK) in water at 25°C in accordance with the manufacturer's operating manual. The presence of FITC doped into the silica shell was confirmed using an inverted fluorescence microscope (TE-2000U, Nikon, Tokyo, Japan).

^{1}H NMR study. The covalent bonding between PEI and FA was ascertained using a VARIAN 400-MHz ^{1}H NMR spectrometer (Varian Inc, Palo Alto, CA). The lyophilized product was dissolved directly in D_2O. PEI and FA were also dissolved in

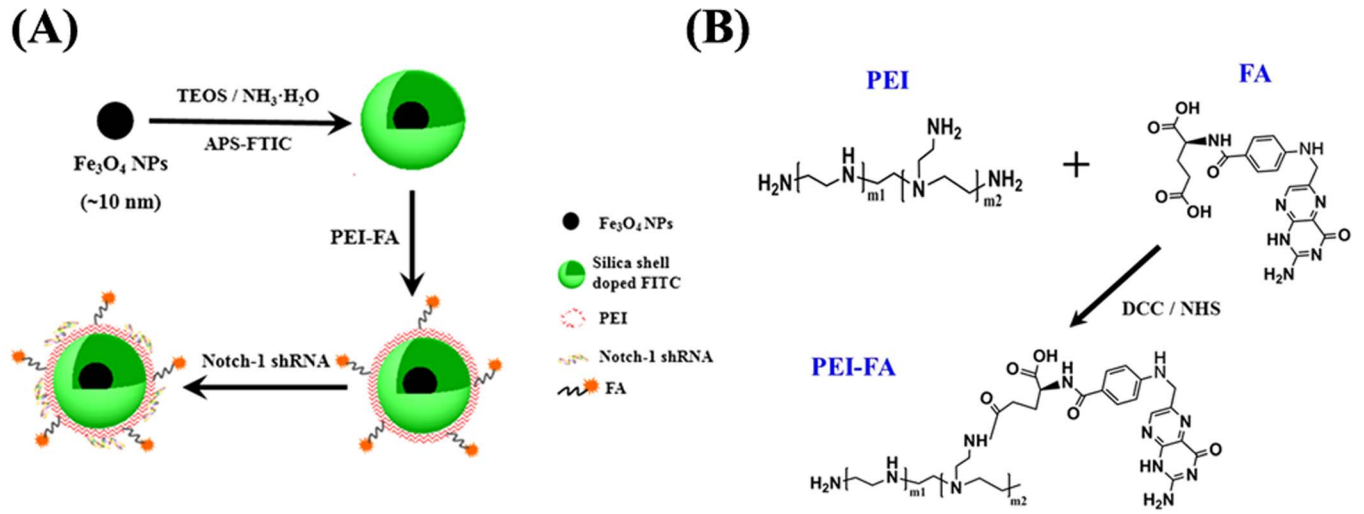

Figure 1 | Synthetic route of folic acid-conjugated PEI-grafted Fe_3O_4@SiO_2(FITC) fluorescent nanoparticles: (A) overview of the synthetic strategy. (B) chemical synthesis of PEI-FA.

D_2O. The production of new bonds was evaluated by the chemical shift of ^1H protons of benzene ring of FA in the range of 6.5–9.0 ppm.

Magnetization curves. Magnetic measurement of samples was performed on a superconducting quantum interference device (SQUID) magnetometer (MPMS XL-7, Quantum Design, San Diego, CA, USA). For measurement, about 10 mg powder of the sample was inserted in a gelatin capsule at room temperature. The magnetic hysteresis loop was measured at room temperature.

Gel retardation assay. To test the absorption ability of Fe_3O_4@SiO_2(FITC)/PEI-FA nanoparticles to Notch-1 shRNA, Notch-1 shRNA was incubated in the Fe_3O_4@SiO_2(FITC)/PEI-FA suspension for 30 min at room temperature to form Fe_3O_4@SiO_2(FITC)/PEI-FA/Notch-1 shRNA nanocomplex by electrostatic absorption at the weight ratios of 5 : 1, 10 : 1, 20 : 1, and 30 : 1. The nanocomplex was confirmed by electrophoresis on a 1% agarose gel with tris/acetate/EDTA buffer at 100 V for 60 min, and visualized by staining with ethidium bromide. The images were acquired using a UV transilluminator (Bio-Rad, Philadelphia, PA, USA).

Notch-1 shRNA stability assay. For the protective effect assay, naked Notch-1 shRNA or Fe_3O_4@SiO_2(FITC)/PEI-FA/Notch-1 shRNA nanocomplex was incubated with DNaseI (1 U/μl) for 30 min. For stability assay in cell culture medium, Fe_3O_4@SiO_2(FITC)/PEI-FA/Notch-1 shRNA nanocomplex at the weight ratio of 20 : 1 or naked Notch-1 shRNA was incubated in L15 culture medium containing 10% FBS for 12, 24, and 48 h. Then treated samples were loaded onto a 1% agarose gel containing 0.01% ethidium bromide and run at 100 V for 60 min. Notch-1 shRNA was released from Fe_3O_4@SiO_2(FITC)/PEI-FA/Notch-1 shRNA nanocomplex by treatment with 1% sodium dodecylsulfate (SDS).

Biocompatibility assay. *Cell viability assay.* Cells were plated at 8000 cells per well in 100 μl of culture medium on 96-well plates. Twenty-four hours after plating, 10, 20, 40 and 80 μg/ml of Fe_3O_4@SiO_2(FITC)/PEI-FA nanoparticles were added to the cells, in triplicate at each concentration, and incubated for 24, 48, and 72 h, respectively. Cell viability was evaluated using the WST-8 cell counting kit (Beyotime, Beijing, China) in accordance with the manufacturer's instructions as previously described[18]. The absorbance was recorded on a microplate reader (Model 680, Bio-Rad, Philadelphia, PA, USA) at a wavelength of 450 nm. Data were expressed as a ratio of treated to untreated cells (control).

Hemolysis assay. Blood from healthy SD rat was collected in heparin-coated tubes as described previously with minor modifications[19,20]. The serum was removed from the blood by centrifugation at 1500 rpm for 5 min, and the red blood cells (RBCs) were then washed three times with sterile isotonic 0.9% NaCl solution. Following the last wash, the RBCs were resuspended with sterile isotonic 0.9% NaCl. The RBC suspension (300 μl) was mixed with 1.2 ml of 10, 20, 40 and 80 μg/ml of Fe_3O_4@SiO_2(FITC)/PEI-FA nanoparticle suspension respectively. Positive and negative controls were also prepared by mixing 300 μl of RBC suspensions with 1.2 ml of deionized water (H_2O) and 0.9% NaCl, respectively. After incubation for 2 h, the samples were then centrifuged for 2 min at 4000 rpm. The absorbance of the supernatant was recorded at 541 nm UV-vis spectroscopy (Hitachi UV-2910, Japan), which is directly proportional to the amount of hemoglobin released.

Evaluation of cellular internalization. MDA-MB-231 cells were seeded on coverslips in a 6-well plate at a seeding density of 5×10^5 cells/well, and the medium was refreshed after 24 h. After treatment with Fe_3O_4@SiO_2(FITC), Fe_3O_4@SiO_2(FITC)/PEI, Fe_3O_4@SiO_2(FITC)/PEI-FA or Fe_3O_4@SiO_2(FITC)/PEI-FA/Notch-1 shRNA nanoparticles, the cells were washed three times with phosphate-buffered saline (PBS, pH 7.4), and then fixed with 4% paraformaldehyde solution in PBS for 15 min at 37°C. The coverslips were then washed three times with PBS to remove nonspecific binding. The cells were further treated with DAPI for 15 min. For FA competition experiments, free FA (1 mM) was preincubated with MDA-MB-231 cells for 2 h prior to addition of Fe_3O_4@SiO_2(FITC)/PEI-FA nanoparticles. All the samples were examined under either an inverted fluorescent microscope (Nikon TE-2000U, Japan) or a confocal laser scanning microscope (TCS SP5, Leica, Germany).

Magnetically targeted delivery assay. MDA-MB-231 cells were seeded in 35-mm culture dishes at 3×10^5 cells per well one day before the experiment. On the second day, 100 μg of Fe_3O_4@SiO_2(FITC)/PEI-FA nanoparticles was added to each dish. *In vitro* magnetically targeted delivery was conducted by placing a magnet under the center of the cell culture dish[21]. After 6 h incubation, the cells were washed three times with sterile PBS. The cellular uptake of Fe_3O_4@SiO_2(FITC)/PEI-FA/Notch-1 shRNA nanocomplex was observed under inverted fluorescent microscope (Nikon TE-2000U, Japan). For cell apoptosis analysis with an external magnetic field, the cells were continued to culture for another 72 h, and then calcein-AM/PI double-staining was performed as described in "*Cell apoptosis assay*" section.

Total RNA isolation and RT-PCR. Total RNA was isolated from cultured MDA-MB-231 cells using the Trizol reagent (Invitrogen, Carlsbad, CA, USA) according to the manufacturer's instructions[22]. One microgram of total RNA from each sample was used for reverse transcription in a 20(μl reaction volume following vendor's instructions. One microliter of each cDNA was used for PCR in a 25(μl reaction. PCR cycling conditions were 30 cycles of 94°C for 1 min, 60°C for 1 min, and 72°C for 2 min. PCR products were resolved on 1% agarose gel with ethidium bromide and the bands were visualized under ultraviolet illumination. Glyceraldehyde 3-phosphate dehydrogenase (GAPDH) was used as an internal control. The primers used for PCR were: Notch-1 (forward, 5(-GGAGCATGTGTAACATCAACA-3′; reverse, 5′CCTCGTACACATTGTAGTT GT-3′; and GAPDH (forward, 5′-GTCTCCTCT GACTTCAACAGCG-3′; reverse, 5′-ACCACCCTGTTGCTGTAGCCAA-3′).

Western blot analysis. After treatment with aforementioned nanoparticles (50 μg/ml), cells were harvested, washed twice with ice-cold PBS, and lysed in a lysis buffer (Beyotime, Beijing, China) containing 20 mM Tris, 150 mM NaCl, 1% Triton X-100 and several protease inhibitors. Total protein concentrations were determined by a bicinchoninic acid protein assay kit (Beyotime, Jiangsu, China). For Western blot analysis[23], an equal amount of lysate (20 μg) was resolved on 10% SDS-PAGE and electrophoretically transferred onto a polyvinylidene difluoride membrane (Millipore Corporation, Bedford, MA, USA). The membranes were blocked with PBST containing 5% skim powder milk for 1 h at room temperature, and then incubated with rabbit anti-human Notch-1 polyclonal antibodies at 1 : 1000 for 1 h at room temperature. After washing, the membranes were further probed with horseradish peroxidase-conjugated goat anti-rabbit IgG at 1 : 5000 dilution. The blots were developed using chemiluminescence (BeyoECL Plus) (Beyotime, Beijing, China).

Cell proliferation assay. For cell proliferation assay, MDA-MB-231 cells were plated in a 96-well plate at a density of 8×10^4 cells/well and grown overnight. Nanoparticles (10 μg/ml) were added to the cells and continued to incubate for 6 h, washed three times with warm PBS (37°C), and growth medium were refreshed. Cell proliferation was measured by WST-8 assay at 24, 48 and 72 h. All experiments were

performed in triplicate. Data were expressed as ratio of treated to the untreated cells (control).

Cell apoptosis assay. Calcein-AM/PI double-staining was used to evaluate apoptotic cell death (red)[24]. MDA-MB-231 cells were seeded in six-well plates (2 ml, 5×10^5 cells/well) and incubated overnight at 37°C to allow the cells to adhere. After treatment with 50 μg/ml aforementioned nanoparticles for 6 h, cells were rinsed with PBS for three times and continued to culture for 72 h. The cells were then stained by a mixture of calcein-AM and PI solution for 10 min. Apoptotic cell death (red) were examined under an inverted fluorescent microscope (Nikon TE-2000U, Japan).

Cellular MR imaging. The day before the experiment, MDA-MB-231 cells were seeded onto 12-well plates at a density of 2×10^5 cells per well. Twenty-four hours after seeding, nanoparticles at a concentration of 25.6 μg/ml were added, and a saline solution without any nanoparticles was used as the control. After 6 h incubation, the cells were washed five times with PBS to remove the non-internalized nanoparticles, harvested, and resuspended in 1 mL PBS for MRI. Fe_3O_4@SiO_2(FITC)/PEI-FA nanoparticles were re-suspended in the cell suspension at iron concentration of 1.6, 3.2, 6.4, 12.8, and 25.6 μg/ml, respectively, and MR imaging was performed at 25°C in a clinical 3.0 Tesla Clinical Siemens Trio scanner (Discovery MR750, GE Healthcare, Boulder, CO, USA). T_2-weighted images were acquired using spin-echo imaging sequences.

Data analysis. All experiments were carried out at least in triplicate. Data were presented as the mean ± standard error of the mean (SEM). The statistical analysis was performed using GraphPad Prism Software version 5.0 (GraphPad Software Inc., San Diego, CA, USA). Statistical significances were determined using the One-way ANOVA followed by Bonferroni tests, and $p < 0.05$ was considered statistically significant.

Results and Discussion

Synthesis and physicochemical characterization of Fe_3O_4@SiO_2(FITC)/PEI-FA/Notch-1 shRNA nanocomplex. The synthetic route for PEI-FA coated Fe_3O_4@SiO_2 nanoparticles is shown in Figure 1. The oleic acid-stabilized Fe_3O_4 nanoparticles were first coated with TEOS and APS-FITC to form a fluorescent silica shell. PEI-FA was then electronically absorbed to the surface of Fe_3O_4@SiO_2(FITC) nanoparticles to enable Fe_3O_4@SiO_2(FITC) nanoparticles to target cancer cells because folate receptor is over-expressed in a wide variety of tumors including breast, lung, and cervical cancer[15,25,26]. We have previously shown that FA provides a good cancer cell-specific target *in vitro*[27]. The modification of Fe_3O_4@SiO_2 presented here also leads a high positively charged surface of the nanoparticles, which enable to load more negatively charged DNA or RNA by electronic absorption. Furthermore, an improved microemulsion method was employed to create the Fe_3O_4@SiO_2(FITC)/PEI-FA nanoparticles for gene delivery.

Scanning electron observations revealed that the Fe_3O_4@SiO_2(FITC) nanoparticles were uniform and averaged 64 nm in diameter (Figures 2A), and that PEI-FA modification and Notch-1 shRNA complexation did not affect the morphology and size distribution of the nanoparticles, but showed a slight tendency to aggregate in solution (Figures 2B and C), which might be caused by the increased surface charge of the particles and Notch-1 shRNA cross-linking. The Fe_3O_4@SiO_2(FITC)/PEI-FA/Notch-1 shRNA nanoparticles could be briefly treated with ultrasonication under acidic solution condition to reduce the aggregation of particles (data not shown). TEM indicated that the magnetic nanocrystal embedded in silica retained its original crystallinity after silica coating and surfactant extraction (Figure 2A, insert). The uniform silica coating of the Fe_3O_4 nanocrystal was further confirmed by EDX method (Figure 2D). The presence of silica and iron in the nanocomposite indicates that core/shell Fe_3O_4@SiO_2 structure is formed. Compared to the Fe_3O_4@SiO_2(FITC) nanoparticles (See Figure S1 in supporting information), the Fe_3O_4@SiO_2(FITC)/PEI-FA nanoparticles have a better dispersity in PBS at room temperature as Fe_3O_4@SiO_2(FITC)/PEI-FA nanoparticles remained well dispersed after 12 h, suggesting that the surface modification of Fe_3O_4@SiO_2(FITC) with PEI-FA improved their dispersity. Furthermore, all the nanoparticles moved to the bottom of the tube soon after the magnet was placed, which also demonstrated that the core-shell nanoparticles were successfully

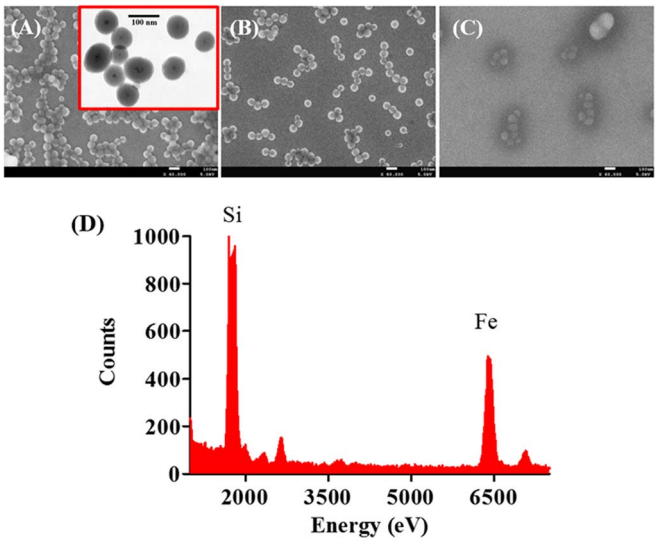

Figure 2 | SEM images of (A) Fe_3O_4@SiO_2(FITC), (B) Fe_3O_4@SiO_2(FITC)/PEI-FA and (C) Fe_3O_4@SiO_2(FITC)/PEI-FA/Notch-1 shRNA nanoparticles. Insert: TEM image shows an average overall size of 64 nm, and 10 nm Fe_3O_4 nanoparticle core. (D) EDX of Fe_3O_4@SiO_2(FITC) showing the presence of Fe_3O_4.

synthesized, and the resultant nanocomposites can be manipulated by an external magnetic field.

FITC-APS conjugates were prepared in advance via an addition reaction between the isothiocyanate group of FITC dye and the primary amine group of APS. This synthetic process enables the co-encapsulation of Fe_3O_4 nanoparticles and a large number of FITC dye molecules to stay together within the silica shell[4,28,29]. Using fluorescence microscopy, we confirmed that both Fe_3O_4@SiO_2(FITC) and Fe_3O_4@SiO_2(FITC)/PEI-FA nanoparticles were well-dispersed, and distinct fluorescence existed for the two nanoparticles (Figure 3). It indicated that PEI-FA modification had no obvious influence on fluorescence intensity (Figure 3B). The ^{1}H NMR analysis was used to determine the composition of the resulting polymers. In the ^{1}H-NMR spectrum of PEI-FA in D_2O as shown in Figure 4A, the signals at δ 2.0–3.0 ppm were attributed to the methylene group in PEI, and the signals at δ 6.5–9.0 related to the H of benzene ring in FA[30,31]. The results indicate that about one FA molecular chain was conjugated to one PEI molecular chain. To verify whether the PEI-FA co-polymer were coated on the surface of Fe_3O_4@SiO_2(FITC) nanoparticles, fluorescence emission spectra were used and the results showed an emission peak at the wavelength of approximately 440 nm for the Fe_3O_4@SiO_2(FITC)/PEI-FA nanoparticle suspension (Figure 4B), which is the characteristic fluorescence emission peak of FA[4,10,31], suggesting that PEI-FA molecules were successfully coated onto the surface of Fe_3O_4@SiO_2(FITC) nanoparticles. The zeta potential analysis further showed a positive surface charge of +17.5 ± 1.3 mV (Figure 4C) for the Fe_3O_4@SiO_2(FITC)/PEI-FA nanoparticle, suggesting that the Fe_3O_4@SiO_2(FITC)/PEI-FA nanoparticle could bind to the negatively charged Notch-1 shRNA through electrostatic interaction. For assessment of the magnetic properties and sensitivity of the formulated nanoparticles, magnetic hysteresis loops were recorded using a magnetometer, and the three types of nanoparticles showed superparamagnetic behavior without magnetic hysteresis (Figure 5) at room temperature (about 300 K). They were found to have no coercive fields, thereby confirming their superparamagnetic nature. There was also no significant difference in their magnetic hysteresis loops and magnetization saturation values even when the Fe_3O_4@SiO_2(FITC)/PEI-FA nanoparticles were modified with the Notch-1 shRNA.

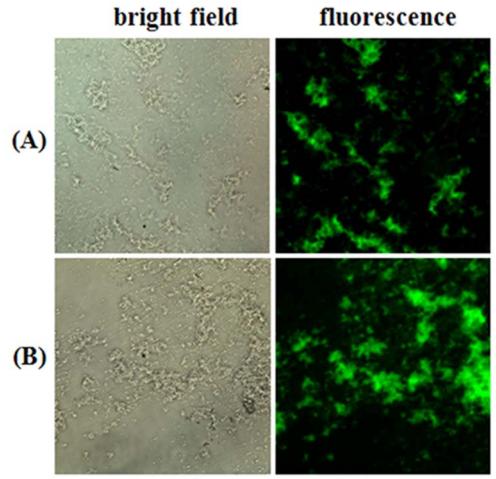

Figure 3 | **Light and fluorescence micrographs of aqueous suspension of (A) Fe_3O_4@SiO_2(FITC) and (B) Fe_3O_4@SiO_2(FITC)/PEI-FA nanoparticles in PBS solution.**

Biological characterizations of Fe_3O_4@SiO_2(FITC)/PEI-FA/Notch-1 shRNA nanocomplex. The nuclear acid stability and nuclear acid-binding capability of the nanoparticles are two very important factors to consider in choosing a gene delivery carrier[32,33]. The condensed form of the nanoparticles/gene complex can protect the nuclear acid from degradation when they pass through cell barriers during gene delivery. In order to study shRNA stability and condensation capabilities of nanoparticles with shRNA, agarose gel electrophoresis was performed. Complexation of nucleic acids with cationic polymers is driven by electrostatic neutralization, during which nucleic acids partially or completely loses negative charge and, consequently, loses mobility in electric field[30,34]. Therefore, by observing he motility of Notch-1 shRNA in gel electrophoresis one can determine Fe_3O_4@SiO_2(FITC)/PEI-FA ability to complex with Notch-1 shRNA. With the increasing of NPs/pDNA weight ratio from 5 : 1 to 30 : 1, the electrophoretic mobility of the Notch-1 shRNA gradually retarded, indicating the enhanced binding of Fe_3O_4@SiO_2(FITC)/PEI-FA nanoparticles to Notch-1 shRNA. When the NPs/shRNA weight ratio reached 15 : 1, no free Notch-1 shRNA bands were observed on the gel, indicating that Notch-1 shRNA had completely complexed with the Fe_3O_4@SiO_2(FITC)/PEI-FA nanoparticles (Figure 6A). We also used DNaseI to further investigate the stability and protection of NPs/shRNA. We found that naked Notch-1 shRNA was completely degraded by DNaseI within 30 min, while Notch-1 shRNA retained in the gel wells by Fe_3O_4@SiO_2(FITC)/PEI-FA binding showed no signs of DNaseI degradation (Figure 6B), demonstrating that PEI-FA could concentrate and wrap

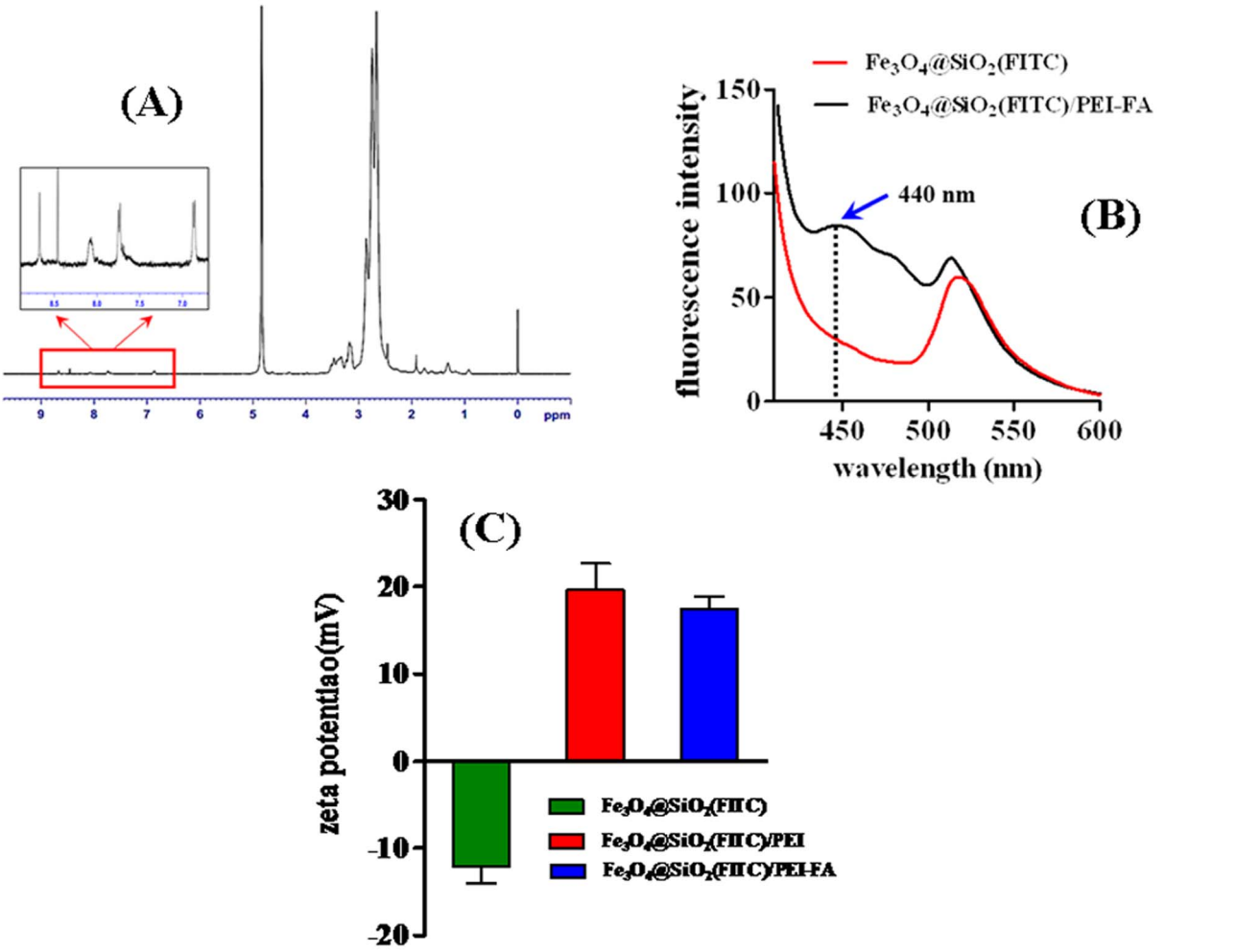

Figure 4 | (A) ^{1}H NMR spectra (300 MHz) of Fe_3O_4@SiO_2(FITC)/PEI-FA nanoparticles in D_2O. (B) Fluorescence emission spectra of Fe_3O_4@SiO_2(FITC) and Fe_3O_4@SiO_2(FITC)/PEI-FA nanoparticles. The fluorescence excitation peak was at a wavelength of approximately 440 nm indicating the successful coupling of PEI-FA to the particle surfaces. (C) Zeta potential measurements of Fe_3O_4@SiO_2(FITC), Fe_3O_4@SiO_2(FITC)/PEI and Fe_3O_4@SiO_2(FITC)/PEI-FA nanoparticles in aqueous suspension.

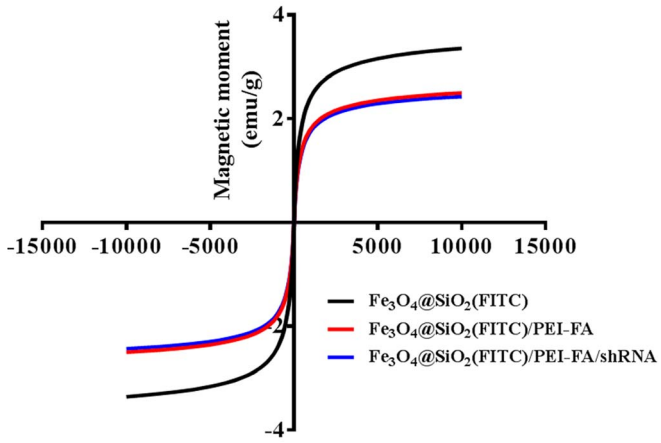

Figure 5 | Field dependent magnetization at 25°C for Fe_3O_4@SiO_2(FITC), Fe_3O_4@SiO_2(FITC)/PEI-FA, and Fe_3O_4@SiO_2(FITC)/PEI-FA/Notch-1 shRNA nanoparticles.

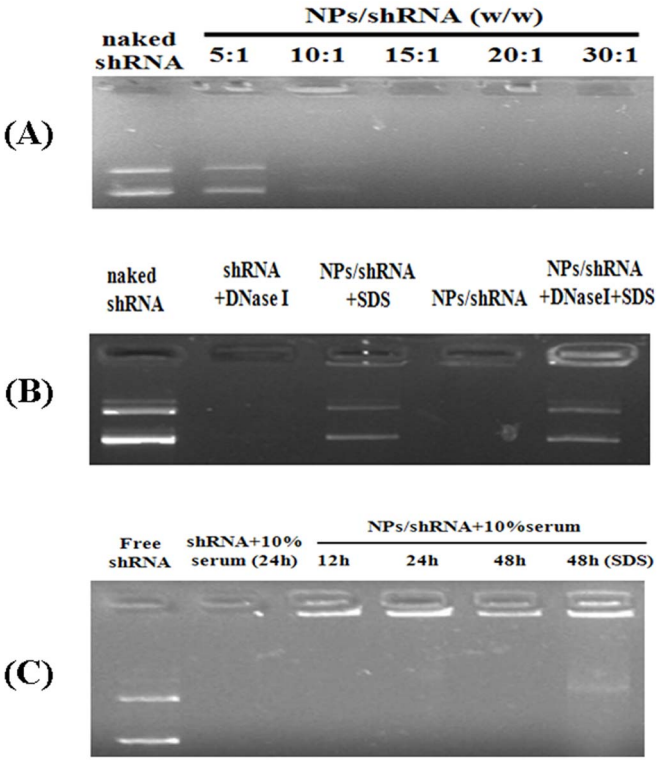

Figure 6 | Notch-1 shRNA stability and binding capability assay. (A) Coupling of Notch-1 shRNA to the surface of Fe_3O_4@SiO_2(FITC)/PEI-FA nanoparticles (NPs) at various weight ratios of NPs to shRNA. (B) Notch-1 shRNA nuclease protection assay. The degradation of Notch-1 shRNA exposed to DNase I for 30 min was observed for naked Notch-1 shRNA, whereas the shRNA in Fe_3O_4@SiO_2/PAH/Notch-1 shRNA nanocomplex at NPs/shRNA weight ratios of 20 : 1 was protected from DNaseI degradation. Shown was Notch-1 shRNA released from dendrimer by 1% SDS and run on a 1% agarose gel. (C) The time-dependent degradation of nuclear acid exposed to 10% serum was observed for naked Notch-1 shRNA and the shRNA in Fe_3O_4@SiO_2/PAH/Notch-1 shRNA nanocomplex remains intact at the NPs/shRNA weight ratio of 20 : 1.

Notch-1 shRNA to protect it from exposure to these agents such as nucleases or other destructive enzymes. Moreover, when naked Notch-1 shRNA or Fe_3O_4@SiO_2(FITC)/PEI-FA/Notch-1 shRNA nanocomplex (NPs/shRNA) were incubated in L15 cell culture medium containing 10% serum from 12 to 48 h, naked Notch-1 shRNA was completely degraded and could not be visualized in the agarose gel, whereas NPs/shRNA nanocomplex could still be visualized in the gel even after incubation for 48 h, demonstrating that Fe_3O_4@SiO_2(FITC)/PEI-FA/Notch-1 shRNA nanocomplex could protect Notch-1 shRNA from serum degradation. Taken together, these results proved that the Fe_3O_4@SiO_2(FITC)/PEI-FA nanoparticles can be used to as an efficient gene carrier.

For the ultimate use of the nanoparticles as gene carrier, it is critical that these nanoparticles after coating with silica and PEI-FA retain their low toxicity, *i.e.*, the gene carrier should not induce cytotoxic effects[35–37]. In order to evaluate the cytotoxicity of resulting nanoparticles, the viability of human breast cancer MDA-MB-231 cells was tested in the presence of Fe_3O_4@SiO_2(FITC)/PEI-FA, Fe_3O_4@SiO_2(FITC)/PEI-FA/scrambled shRNA, or equal volume of cell culture medium as a control. As shown in figure 7, both Fe_3O_4@SiO_2(FITC)/PEI-FA and Fe_3O_4@SiO_2(FITC)/PEI-FA/scrambled shRNA nanoparticles showed no significant cytotoxicity compared to control cells. To better define the biocompatibility of the nanocomplex as gene carrier, a hemolysis assay was conducted to evaluate its compatibility in blood. During the hemolysis assay, hemoglobin released into the solution is direct proportional to hemolytic activity of the carrier, therefore the absorbance 541 nm can be used to quantify the hemolytic activity[20]. As shown in Figure 8, no visible hemolysis can be observed for Fe_3O_4@SiO_2(FITC)/PEI-FA nanoparticles at 80 mg/ml. Quantitative analysis by UV-vis spectroscopy also showed that Fe_3O_4@SiO_2(FITC)/PEI-FA nanoparticles had negligible hemolytic activity.

Cellular uptake of Fe_3O_4@SiO_2(FITC)/PEI-FA/Notch-1 shRNA nanocomplex into human breast cancer cells. *In vitro* cellular uptake experiments were performed using human breast carcinoma MDA-MB-231 cells, known to significantly overexpress the folate receptor[15,25,26]. The uptake of the nanoparticle conjugates was evaluated after 6-h cell culture, and is shown in Figure 9. In contrast to Fe_3O_4@SiO_2(FITC) or Fe_3O_4@SiO_2(FITC)/PEI, the uptake of FA-conjugated Fe_3O_4@SiO_2(FITC)/PEI-FA by MDA-MB-231 cells was ~3-fold higher than those cultured with Fe_3O_4@SiO_2(FITC). PEI, a cationic polymer, could also facilitate nanoparticle uptake in some extent. While the increase in intracellular Fe_3O_4@SiO_2(FITC)/PEI nanoparticles was somewhat visible, however, the fluorescent intensity was considerably less than that in FA-conjugated Fe_3O_4@SiO_2(FITC)/PEI-FA nanoparticles. Furthermore, high uptake was also observed in Fe_3O_4@SiO_2(FITC)/PEI-FA/Notch-1 shRNA nanocomplex (Figure 10), which demonstrated that absorption of Notch-1 shRNA to the nanoparticles did not affect uptake. To ascertain that the nanoparticles were indeed internalized rather than being bound to cell membrane, MDA-MB-231 cells incubated with various nanoparticles were examined by confocal fluorescence microscopy. As shown in Figure 10, the nanoparticles mainly localized to the cytoplasm after 6 h culture. These results agreed well with that of inverted fluorescence microscopy, and also confirmed that the uptake of FA-conjugated Fe_3O_4@SiO_2(FITC)/PEI-FA nanoparticles was more favorable than other non-FA-conjugated nanoparticles.

The specific targeting of the folate receptor by Fe_3O_4@SiO_2(FITC)/PEI-FA nanoparticles was further verified by a competitive inhibition assay, in which MDA-MB-231 cells were pretreated with free FA before culturing with Fe_3O_4@SiO_2(FITC)/PEI-FA nanoparticles. As expected, a sharp decreased uptake of the nanoparticles by MDA-MB-231 cells was observed (Figure 10). This result indicates that the uptake of Fe_3O_4@SiO_2(FITC)/PEI-FA nanoparticles was mediated by folate receptor on the cell surface[9,38]. Taken together, these findings indicated that conjugation of Fe_3O_4@SiO_2(FITC) nanoparticles with a tumor targeting agent, FA specif-

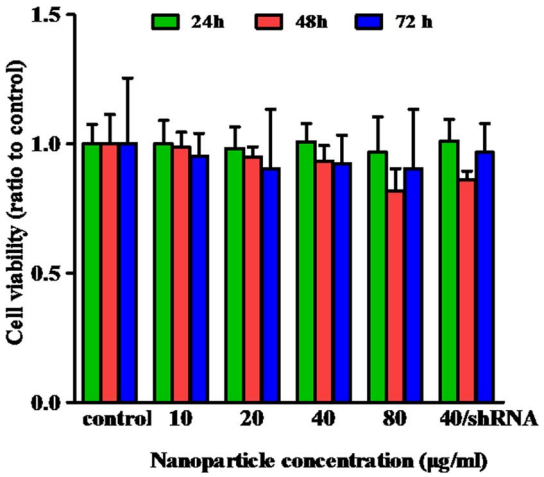

Figure 7 | Viability of human breast cancer MDA-MB-231 cells after incubation with various concentrations of Fe_3O_4@SiO_2(FITC)/PEI-FA nanoparticles or Fe_3O_4@SiO_2(FITC)/PEI-FA/scrambled shRNA nanoparticles at 24, 48 and 72 h. Data are presented as means ± SEM (n = 3).

ically, led to the increased targeted uptake of Fe_3O_4@SiO_2(FITC)/PEI-FA nanoparticles by MDA-MB-231 cells bearing FA receptor.

Silencing Notch-1 gene expression and anti-tumor effect of Fe_3O_4@SiO_2(FITC)/PEI-FA/Notch-1 shRNA nanocomplex. To evaluate the Notch-1 gene silencing effect of Fe_3O_4@SiO_2(FITC)/PEI-FA/Notch-1 shRNA nanocomplex, human breast carcinoma cells (MDA-MB-231) were incubated with the nanoparticles as described in materials and methods. As shown in Figure S2 (see Supporting Information), Fe_3O_4@SiO_2(FITC)/PEI-FA/Notch-1 shRNA nanocomplex efficiently decreased the expression of Notch-1 at both mRNA and protein level in MDA-MB-231 cells compared to that in nanoparticles containing either a scrambled shRNA or untransfected cells. These results suggest that the Fe_3O_4@SiO_2(FITC)/PEI-FA/Notch-1 shRNA nanocomplex could silence Notch-1 expression in a highly sequence-specific fashion[39,40].

We then investigated whether these nanoparticles have any effect on cell proliferation. Cells were treated with various nanoparticles for

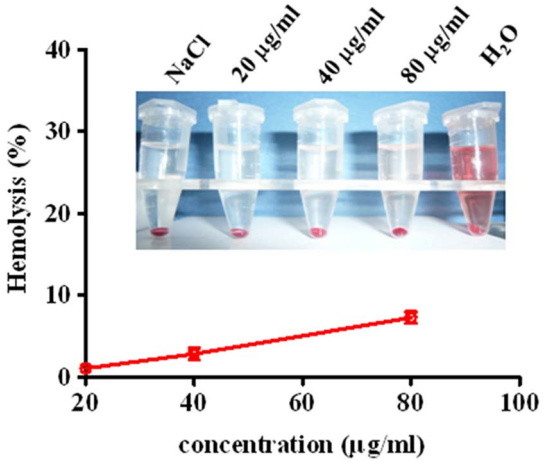

Figure 8 | Hemolysis assay of Fe_3O_4@SiO_2(FITC)/PEI-FA nanoparticles at different concentrations, 0.9% NaCl and H_2O were used as negative and positive control, respectively. The mixtures were centrifuged to detect the presence of red color in the supernatant, the absorbance of which is proportional to the amount of hemoglobin released from the red blood cells.

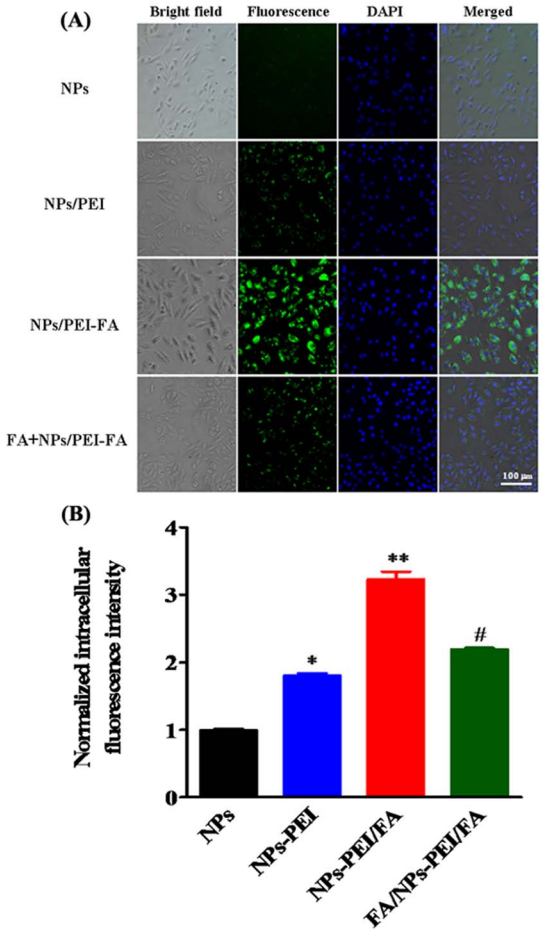

Figure 9 | (A) Cellular internalization of nanoparticles into human breast cancer MDA-MB-231 cells was observed by an inverted microscope after 6 h incubation with Fe_3O_4@SiO_2(FITC) (NPs), Fe_3O_4@SiO_2(FITC)/PEI (NPs/PEI), Fe_3O_4@SiO_2(FITC)/PEI-FA (NPs/PEI-FA), and FA pretreated MDA-MB-231 cells before Fe_3O_4@SiO_2(FITC)/PEI-FA addition (FA + NPs/PEI-FA). (B) Quantitative cellular uptake of the nanoparticles into MDA-MB-231 cells through measuring mean fluorescence intensity of FITC fluorescence in the cells, which was normalized to the control (NPs) (n = 5, mean ± SD). *$p < 0.05$ compared with NPs, **$p < 0.01$ compared with NPs, $^{\#}p < 0.05$ compared with NPs/PEI-FA.

24, 48 and 72 h, and it showed that Fe_3O_4@SiO_2(FITC)/PEI-FA/Notch-1 shRNA nanocomplex inhibited MDA-MB-231 cell proliferation, especially at 48 and 72 h (Figure 11). To evaluate whether the inhibition of cell proliferation by Fe_3O_4@SiO_2(FITC)/PEI-FA/Notch-1 shRNA nanocomplex was due to its apoptotic effect, the cell apoptosis was evaluated by calcein-AM/PI double staining. As shown in Figure 12, more cell apoptotic cells were observed in cells treated with Fe_3O_4@SiO_2(FITC)/PEI-FA/Notch-1 shRNA nanocomplex compared to control treatment. These data suggest that the inhibited cell proliferation induced by Fe_3O_4@SiO_2(FITC)/PEI-FA/Notch-1 shRNA nanocomplex was at least partially attributed to its apoptotic effect. Notch-1 signaling pathway is an evolutionarily conserved signaling pathway that has been shown to regulate many cellular processes including cell proliferation, differentiation, apoptosis, and survival[41,42]. In light of the previous finding that silencing Notch-1 promoted cancer cell apoptosis[24,42], our data indicate that Fe_3O_4@SiO_2(FITC)/PEI-FA/Notch-1 shRNA nanocomplex can be used as an efficient gene carrier for targeted killing of cancer cells bearing folate receptor.

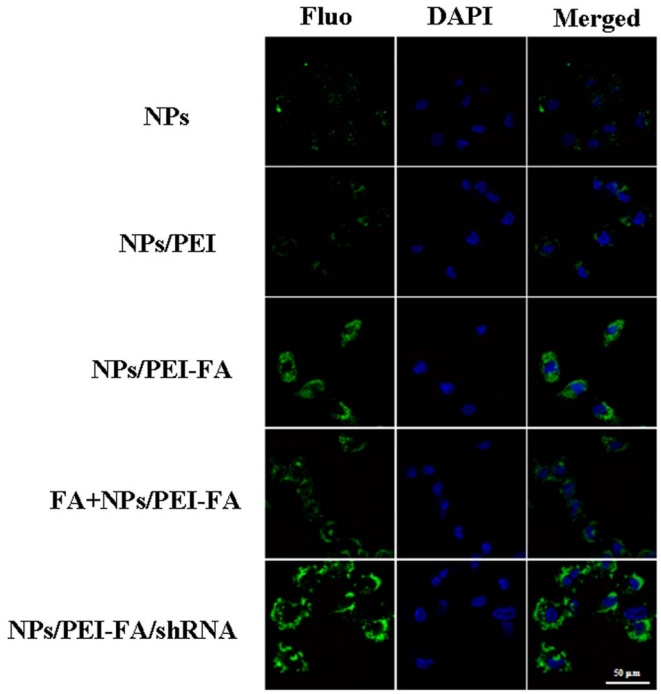

Figure 10 | Confocal laser scanning microscopy images of MDA-MB-231 cells after 6 h incubation with indicated nanoparticles. The internalized nanoparticles were green (FITC) and nuclei were blue (DAPI staining).

Besides the folate receptor-mediated molecular targeting, the magnetic property of Fe_3O_4@SiO_2(FITC)/PEI-FA/Notch-1 shRNA nanocomplex could be also utilized for magnetically targeted delivery. When MDA-MB-231 cells were incubated with Fe_3O_4@SiO_2(FITC)/PEI-FA/Notch-1 shRNA nanocomplex for 6 h, instead of 72 h for apoptosis assay, in the presence of a magnetic field under the center of the cell culture dish (Figure 13A), the uptake of the nanoparticles (green cells) by cells near the magnet was significantly higher than those far from the magnet (Figure 13B). Accordingly, the cells near the magnet showed apoptotic phenotype (red) compared to those far from the magnet (Figure 13C). Collectively, our data demonstrated that Fe_3O_4@SiO_2(FITC)/PEI-FA/Notch-1 shRNA nanocomplex is an efficient gene delivery system possessing both molecular targeting and magnetic targeting capabilities.

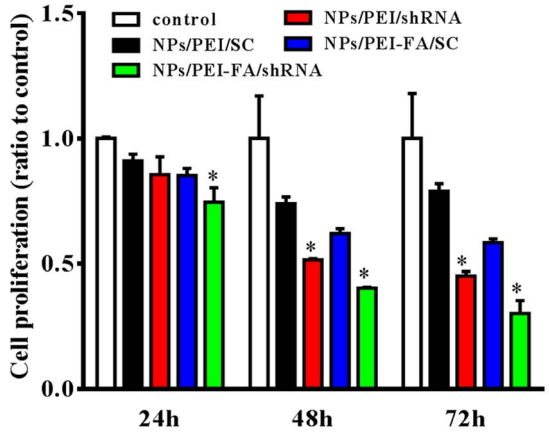

Figure 11 | Cell proliferation assay of human breast cancer MDA-MB-231 cells treated with Fe_3O_4@SiO_2(FITC) (control), Fe_3O_4@SiO_2(FITC)/PEI/Notch-1 shRNA (NPs/PEI/shRNA), Fe_3O_4@SiO_2(FITC)/PEI/scrambled shRNA (NPs/PEI/SC), Fe_3O_4@SiO_2(FITC)/PEI-FA/scrambled shRNA (NPs/PEI-FA/SC), or Fe_3O_4@SiO_2(FITC)/PEI-FA/Notch-1 shRNA (NPs/PEI-FA/shRNA). $^*p < 0.05$ compared with control.

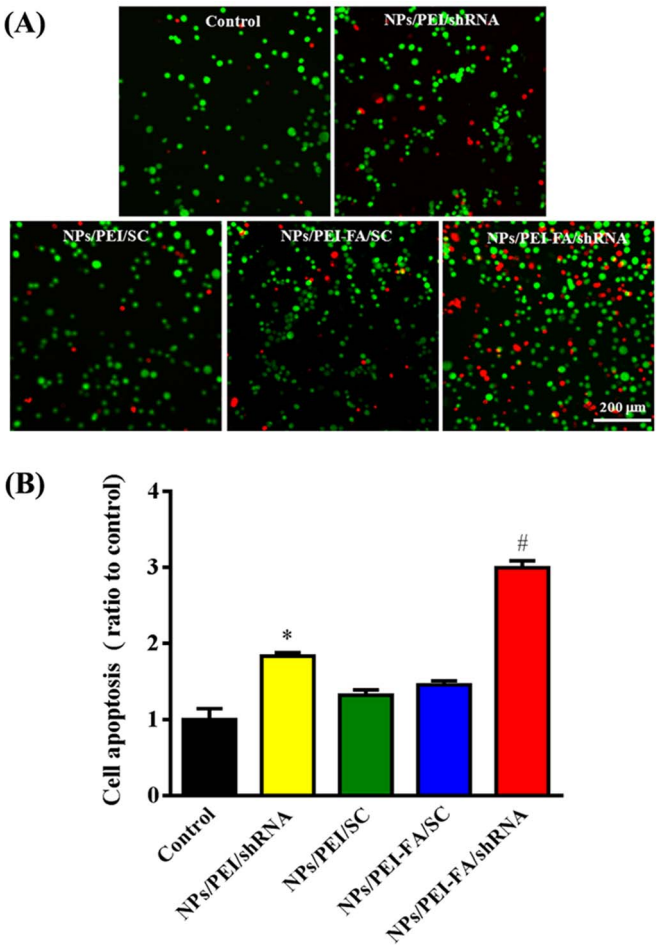

Figure 12 | Cell apoptosis assay by calcein-AM/PI double staining. (A) Representative images show cells incubated with: equal volume culture medium (control), Fe_3O_4@SiO_2(FITC)/PEI/Notch-1 shRNA (NPs/PEI/shRNA), Fe_3O_4@SiO_2(FITC)/PEI/scrambled shRNA (NPs/PEI/SC), Fe_3O_4@SiO_2(FITC)/PEI/scrambled shRNA (NPs/PEI-FA/SC), or Fe_3O_4@SiO_2(FITC)/PEI-FA/Notch-1 shRNA (NPs/PEI-FA/shRNA). (B) Quantitative analysis of cell apoptosis was evaluated from more than six micrographs by calculating the fluorescence intensity of PI (red) and then normalized to the control. $^*P < 0.05$ NPs/PEI/siRNA *vs.* control or NPs/PEI/SC; $^{\#}P < 0.01$ NPs/PEI-FA/siRNA *vs.* NPs/PEI-FA/SC.

MR imaging of cells after nanoparticle internalization. To evaluate the potential of Fe_3O_4@SiO_2(FITC)/PEI-FA/Notch-1 shRNA nanocomplex to be used as a targeted MR contrast agent, MDA-MB-231 cells were cultured with Fe_3O_4@SiO_2(FITC), Fe_3O_4@SiO_2(FITC)/PEI, Fe_3O_4@SiO_2(FITC)/PEI-FA or Fe_3O_4@SiO_2(FITC)/PEI-FA/Notch-1 shRNA as described in materials and methods. Cells were harvested and resuspended in PBS and the T_2-weighted MR phantom images were obtained. As shown in Figure 14, cells incubated with Fe_3O_4@SiO_2(FITC)/PEI-FA or Fe_3O_4@SiO_2(FITC)/PEI-FA/Notch-1 shRNA showed a significant negative contrast enhancement (signal darkening) over other cells. As the concentration of the Fe_3O_4@SiO_2(FITC)/PEI-FA/Notch-1 shRNA nanocomplex increases, the T_2-weighted MR image becomes darker for MDA-MB-231 cells, suggesting that the nanocomplex could also be used as a probe for T_2 MR imaging. Our data demonstrated that Fe_3O_4@SiO_2(FITC)/PEI-FA/Notch-1 shRNA nanocomplex can be exploited as a novel theranostic for cancer gene therapy and imaging probe for cancer diagnosis.

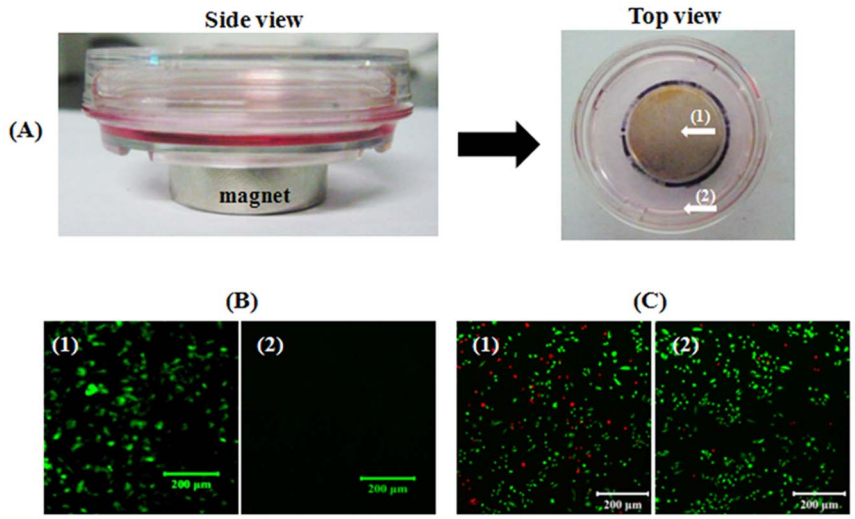

Figure 13 | Magnetically targeted delivery of Fe_3O_4@SiO_2(FITC)/PEI-FA/Notch-1 shRNA nanocomplex. (A) Photos of MDA-MB-231 cells incubated with Fe_3O_4@SiO_2(FITC)/PEI-FA/Notch-1 shRNA nanocomplex in the presence of a magnet. (B) Cellular uptake of Fe_3O_4@SiO_2(FITC)/PEI-FA/Notch-1 shRNA nanocomplex (green) at different positions of the cell culture dish as indicated. (C) Fluorescence images of calcein-AM (green)/PI (red) double-stained cells at different positions of the cell culture dish as indicated. The number of cells showing both uptake of the nanoparticles and apoptosis near the magnet were significantly higher than that of cells far away from the magnet.

Conclusions

In summary, a multifunctional Fe_3O_4@SiO_2(FITC)/PEI-FA/Notch-1 shRNA nanocomplex with specific targeting ability is developed. The multifunctional nanocomplex was stable and dispersed in aqueous solution, and showed minimal cytotoxicity, and possesses dual functions as both a gene delivery vehicle and a MR imaging contrast agent. The cellular uptake of the nanocomplex was significantly enhanced in the folate receptor overexpressed human breast cancer cell lines (MDA-MB-231). Moreover, the cell proliferation treated by Fe_3O_4@SiO_2(FITC)/PEI-FA/Notch-1 shRNA nanocomplex was significantly inhibited, contributing to the increased intracellular delivery of Notch-1 shRNA and subsequently down-regulating the Notch-1 expression to inhibit the Notch-1 signal pathway. Although the *in vivo* therapeutic effects should be further investigated, based on the *in vitro* data and findings, Fe_3O_4@SiO_2(FITC)/PEI-FA/Notch-1 shRNA nanocomplex presented here may be exploited as a theranostic candidate for human breast cancer gene therapy and diagnosis.

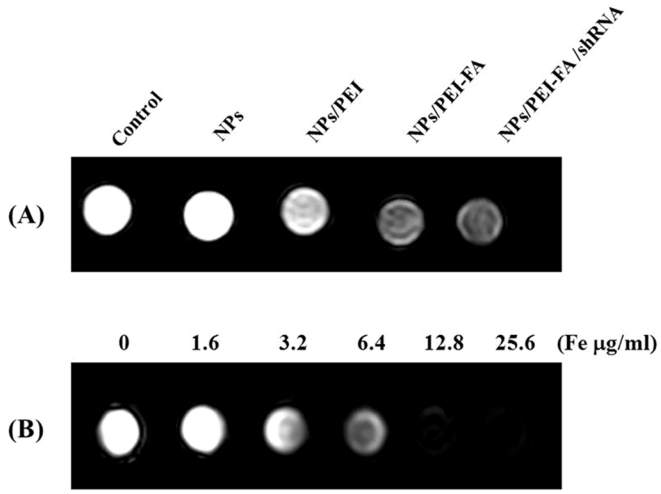

Figure 14 | T_2-weighted imaging of MDA-MB-231 cells. (A) MR images of phantoms containing MDA-MB-231 cells after 6 h incubation with Fe_3O_4@SiO_2(FITC) (NPs), Fe_3O_4@SiO_2(FITC)/PEI (NPs/PEI), Fe_3O_4@SiO_2(FITC)/PEI-FA (NPs/PEI-FA) or Fe_3O_4@SiO_2(FITC)/PEI-FA/Notch-1 shRNA (NPs/PEI-FA/shRNA) at a concentration of 25.6 μg/ml. (B) T_2-weighted MR images of Fe_3O_4@SiO_2(FITC)/PEI/Notch-1 shRNA nanocomplex aqueous solutions at different Fe concentrations. A saline solution without any nanoparticles was used as the control group.

1. Kim, S. H. *et al.* Local and systemic delivery of VEGF siRNA using polyelectrolyte complex micelles for effective treatment of cancer. *J. Control. Release* **129**, 107–116 (2008).
2. Han, L. *et al.* Enhanced siRNA delivery and silencing gold-chitosan nanosystem with surface charge-reversal polymer assembly and good biocompatibility. *ACS Nano* **6**, 7340–7351 (2012).
3. Zhang, L. *et al.* Multifunctional fluorescent-magnetic polyethyleneimine functionalized Fe_3O_4-mesoporous silica yolk-shell nanocapsules for siRNA delivery. *Chem. Commun (Camb).* **48**, 8706–8708 (2012).
4. Yang, H. *et al.* VCAM-1-targeted core/shell nanoparticles for selective adhesion and delivery to endothelial cells with lipopolysaccharide-induced inflammation under shear flow and cellular magnetic resonance imaging in vitro. *Int. J. Nanomedicine* **8**, 1897–1906 (2013).
5. Lu, Y., Yin, Y., Mayers, B. T. & Xia, Y. Modifying the surface properties of superparamagnetic iron oxide nanoparticles through a sol−gel approach. *Nano Lett* **2**, 183–186 (2002).
6. Graf, C., vossen, D. L. J., Imhof, A. & van Blaaderen, A. A general method to coat colloidal particles with silica. *Langmuir* **19**, 6693–6700 (2003).
7. Xia, T. *et al.* Polyethyleneimine coating enhances the cellular uptake of mesoporous silica nanoparticles and allows safe delivery of siRNA and DNA constructs. *ACS Nano* **3**, 3273–3286 (2009).
8. Chen, Y. *et al.* Development of an MRI-visible nonviral vector for siRNA delivery targeting gastric cancer. *Int. J. Nanomedicine* **7**, 359–368 (2012).
9. Sun, C., Sze, R. & Zhang, M. Folic acid-PEG conjugated superparamagnetic nanoparticles for targeted cellular uptake and detection by MRI. *J. Biomed. Mater. Res. A.* **78**, 550–557 (2006).
10. Zhu, Y., Fang, Y. & Kaskel, S. Folate-conjugated Fe_3O_4@SiO_2 hollow mesoporous spheres for targeted anticancer drug delivery. *J. Phys. Chem. C.* **114**, 16382–16388 (2010).
11. Low, P. S., Henne, W. A. & Doorneweerd, D. D. Discovery and development of folic-acid-based receptor targeting for imaging and therapy of cancer and inflammatory diseases. *Acc. Chem. Res.* **41**, 120–129 (2008).
12. Pan, X. & Lee, R. J. Tumour-selective drug delivery via folate receptor-targeted liposomes. *Expert Opin. Drug Deliv.* **1**, 7–17 (2004).
13. Sudimack, J. & Lee, R. J. Targeted drug delivery via the folate receptor. *Adv. Drug Deliv. Rev.* **41**, 147–162 (2000).
14. Ridgway, J. *et al.* Inhibition of Dll4 signalling inhibits tumour growth by deregulating angiogenesis. *Nature* **444**, 1083–1087 (2006).
15. Mamaeva, V. *et al.* Mesoporous silica nanoparticles as drug delivery systems for targeted inhibition of Notch signaling in cancer. *Mol. Ther.* **19**, 1538–1546 (2011).

16. Zhang, G. *et al*. Fluorescent magnetic nanoprobes: design and application for cell imaging. *J. Colloid. Interface. Sci.* **351**, 128–133 (2010).
17. Liu, Y. *et al*. Multifunctional nanoparticles of Fe(3)O(4)@SiO(2)(FITC)/PAH conjugated the recombinant plasmid of pIRSE2-EGFP/VEGF(165) with dual functions for gene delivery and cellular imaging. *Expert Opin. Drug Deliv.* **9**, 1197–1207 (2012).
18. Shi, M. *et al*. Core/shell Fe_3O_4 @SiO_2 nanoparticles modified with PAH as a vector for EGFP plasmid DNA delivery into HeLa cells. *Macromol. Biosci.* **11**, 1563–1569 (2011).
19. Slowing, II, Wu, C. W., Vivero-Escoto, J. L. & Lin, V. S. Mesoporous silica nanoparticles for reducing hemolytic activity towards mammalian red blood cells. *Small* **5**, 57–62 (2009).
20. Guo, L. *et al*. Hollow mesoporous carbon spheres-an excellent bilirubin adsorbent. *Chem. Commun (Camb).* **40**, 6071–6073 (2009).
21. Shi, X. *et al*. Graphene-based magnetic plasmonic nanocomposite for dual bioimaging and photothermal therapy. *Biomaterials* **34**, 4786–4793 (2013).
22. Meng, G., Liu, Y., Lou, C. & Yang, H. Emodin suppresses lipopolysaccharide-induced pro-inflammatory responses and NF-kappaB activation by disrupting lipid rafts in CD14-negative endothelial cells. *Br. J. Pharmacol.* **161**, 1628–1644 (2010).
23. Zhao, F. *et al*. Roles for GP IIb/IIIa and alpha(v)beta(3) integrins in MDA-MB-231 cell invasion and shear flow-induced cancer cell mechanotransduction. *Cancer Lett.* **344**, 62–73 (2014).
24. Li, L. *et al*. Notch-1 Signaling Promotes the Malignant Features of Human Breast Cancer through NF-kappaB Activation. *PLoS One* **9**, e95912 (2014).
25. Meier, R. *et al*. Breast cancers: MR imaging of folate-receptor expression with the folate-specific nanoparticle P1133. *Radiology* **255**, 527–535 (2010).
26. Cui, S. *et al*. In vivo targeted deep-tissue photodynamic therapy based on near-infrared light triggered upconversion nanoconstruct. *ACS Nano* **7**, 676–688 (2013).
27. Yang, H. *et al*. Investigation of folate-conjugated fluorescent silica nanoparticles for targeting delivery to folate receptor-positive tumors and their internalization mechanism. *Int. J. Nanomedicine* **6**, 2023–2032 (2011).
28. Lawrier, G. A., Battersby, B. J. & Trau, M. Synthesis of optically complex core-shell colloidal suspensions: pathways to multiplexed biological screening. *Adv Funct Mater* **13**, 887–896 (2003).
29. Lee, J. E. *et al*. Uniform mesoporous dye-doped silica nanoparticles decorated with multiple magnetite nanocrystals for simultaneous enhanced magnetic resonance imaging, fluorescence imaging, and drug delivery. *J. Am. Chem. Soc.* **132**, 552–557 (2010).
30. Zou, S. *et al*. Enhanced apoptosis of ovarian cancer cells via nanocarrier-mediated codelivery of siRNA and doxorubicin. *Int. J. Nanomedicine* **7**, 3823–3835 (2012).
31. Zou, T. *et al*. Synthesis of poly(alpha,beta-[N-(2-hydroxyethyl)-L-aspartamide])-folate for drug delivery. *J. Biomater. Sci. Polym. Ed.* **21**, 759–770 (2010).
32. Son, S. & Kim, W. J. Biodegradable nanoparticles modified by branched polyethylenimine for plasmid DNA delivery. *Biomaterials* **31**, 133–143 (2010).
33. Liu, C. *et al*. The targeted co-delivery of DNA and doxorubicin to tumor cells via multifunctional PEI-PEG based nanoparticles. *Biomaterials* **34**, 2547–2564 (2013).
34. Chen, G. *et al*. MRI-visible polymeric vector bearing CD3 single chain antibody for gene delivery to T cells for immunosuppression. *Biomaterials* **30**, 1962–1970 (2009).
35. Deng, L. *et al*. Development and optimization of doxorubicin loaded poly(lactic-co-glycolic acid) nanobubbles for drug delivery into HeLa cells. *J. Nanosci. Nanotechnol.* **14**, 2947–2954 (2014).
36. Liu, Y. *et al*. Silica nanoparticles as promising drug/gene delivery carriers and fluorescent nano-probes: recent advances. *Curr. Cancer Drug Targets* **11**, 156–163 (2011).
37. Kano, A. *et al*. Grafting of poly(ethylene glycol) to poly-lysine augments its lifetime in blood circulation and accumulation in tumors without loss of the ability to associate with siRNA. *J. Control. Release* **149**, 2–7 (2011).
38. Kumar, M. *et al*. Cellular interaction of folic acid conjugated superparamagnetic iron oxide nanoparticles and its use as contrast agent for targeted magnetic imaging of tumor cells. *Int. J. Nanomedicine* **7**, 3503–3516 (2012).
39. Kim, S. H. *et al*. PEG conjugated VEGF siRNA for anti-angiogenic gene therapy. *J. Control. Release* **116**, 123–129 (2006).
40. Miele, E. *et al*. Nanoparticle-based delivery of small interfering RNA: challenges for cancer therapy. *Int. J. Nanomedicine* **7**, 3637–3657 (2012).
41. Wu, F., Stutzman, A. & Mo, Y. Y. Notch signaling and its role in breast cancer. *Front. Biosci.* **12**, 4370–4383 (2007).
42. Wang, Z. *et al*. Down-regulation of Notch-1 and Jagged-1 inhibits prostate cancer cell growth, migration and invasion, and induces apoptosis via inactivation of Akt, mTOR, and NF-kappaB signaling pathways. *J. Cell. Biochem.* **109**, 726–736 (2010).

Acknowledgments

We would like to thank the financial supports, in whole or in part, by the National Natural Science Foundation of China (11272083, 81201192, 81101147, 31470906, 31470959, 81471785), the Sichuan Youth Science and Technology Foundation of China (2014JQ0008, 2010JQ0004), the Postdoctoral Program of China (2011M501297, 2012T50715), and the Fundamental Research Funds for Central Universities in China (ZYGX2010X019, ZYGX2010J101, ZYGX2011J099).

Author contributions

H.Y., Y.L. and Y.L. conceived and designed the experiments; H.Y., Y.L., T.L., M.X. and Y.C. performed the experiments; H.Y., Y.L., C.W., X.D. and Y.L. analyzed the data; C.W. and Y.L. contributed reagents/materials/analysis tools; H.Y., Y.L., X.D. and Y.L. wrote the paper. All the authors discussed and commented on the manuscript.

Additional information

Supplementary information accompanies this paper at http://www.nature.com/scientificreports

Competing financial interests: The authors declare no competing financial interests.

How to cite this article: Yang, H. *et al*. Multifunctional Core/Shell Nanoparticles Cross-linked Polyetherimide-folic Acid as Efficient Notch-1 siRNA Carrier for Targeted Killing of Breast Cancer. *Sci. Rep.* **4**, 7072; DOI:10.1038/srep07072 (2014).